Biochimica et Biophysica Acta 1834 (2013) 2823–2831

Contents lists available at ScienceDirect

Biochimica et Biophysica Acta

journal homepage: www.elsevier.com/locate/bbapap

Structural and thermodynamic studies of two centrin isoforms from *Blastocladiella emersonii* upon calcium binding

Ana I. Camargo [a], Helton J. Wiggers [a], Julio C.P. Damalio [a], Ana P.U. Araujo [a], Karina F. Ribichich [b,1], Paulo C. de Camargo [c,*]

[a] Instituto de Física de São Carlos, Universidade de São Paulo, São Carlos, SP, Brazil
[b] Instituto de Química de São Paulo, Universidade de São Paulo, São Paulo, SP, Brazil
[c] PIPE, Universidade Federal do Paraná, Curitiba, PR, Brazil

ARTICLE INFO

Article history:
Received 18 February 2013
Received in revised form 30 September 2013
Accepted 6 October 2013
Available online 22 October 2013

Keywords:
Centrins
Blastocladiella emersonii
Calcium-binding protein
EF-hand protein
Isothermal titration calorimetry (ITC)

ABSTRACT

Centrins are calcium-binding proteins associated with microtubules organizing centers. Members of two divergent subfamilies of centrins were found in the aquatic fungus *Blastocladiella emersonii*, contrasting with the occurrence of only one member known for the better explored terrestrial fungi. BeCen1 shows greatest identity with human centrins HsCen1, HsCen2 and green algae centrin CrCenp, while BeCen3 records largest identity with human centrin HsCen3 and yeast centrin Cdc31p. Following the discovery of this unique feature, BeCen1 and BeCen3 centrins were produced to study whether these proteins had distinct features upon calcium binding. Circular dichroism showed opposite calcium binding effects on the α-helix arrangement of the secondary structure. The spectra indicated a decrease in α-helix signal for holo-BeCen1 contrasting with an increase for holo-BeCen3. In addition, only BeCen1 refolds after being de-natured. The fluorescence emission of the hydrophobic probe ANS increases for both proteins likely due to hydrophobic exposure, however, only BeCen1 presents a clear blue shift when calcium is added. ITC experiments identified four calcium binding sites for both proteins. In contrast to calcium binding to BeCen1, which is mainly endothermic, binding to BeCen3 is mainly exothermic. Light-scattering evidenced the formation of large particles in solution for BeCen1 and BeCen3 at temperatures above 30 °C and 40 °C, respectively. Atomic force microscopy confirmed the presence of supramolecular structures, which differ in the compactness and branching degree. Binding of calcium leads to different structural changes in BeCen1 and BeCen3 and the thermodynamic characteristics of the interaction also differ.

1. Introduction

Centrin proteins were first described in the flagellar apparatus of the green alga *Tetraselmis striata* as responsible for the calcium-dependent contraction of fibers. These proteins are also found in a variety of eukaryotic species, including protists [1], green alga [2], fungi [3], plants [4], and animals [5–7]. Centrins are small acid calcium-binding proteins involved in several cellular functions, such as, signal transduction [8], nucleotide excision repair and nucleus cytoplasm messenger ribonucleic acid (mRNA) transport [9], mainly in the context of duplication and segregation of the centrosome in the animal cell and analogous microtubule organizing centers (MTOCs) in other organisms. These calcium-binding proteins are part of the EF-hand superfamily, which is defined by its flexible helix-loop-helix secondary structure that binds calcium [10]. Centrins can be divided into two divergent subfamilies according to their functions and sequence similarity: 1 — characterized by the centrin of the green alga *Chlamydomonas reinhardtii* (CrCenp), mainly responsible for contractile functions; 2 — represented by the centrin of the yeast *Saccharomyces cerevisiae* (Cdc31p), responsible for MTOC duplication [7]. Both, alga and yeast have only one isoform of centrin protein.

Blastocladiella emersonii, a saprobic aquatic fungus belongs to the Blastocladiomycota phylum [11] and grows as a coenocytic cell with basal rhizoids that produce a single zoosporangium, yielding a large number of flagellated zoospores. It can be found in freshwater ponds, streams or ditches, and it is easily maintained in culture. These cultures can be manipulated easily to induce any of the life cycle stages (vegetative or sporulating phases) using the adequate media [12]. Similarly to members of other early phyla, the flagellated phase of this fungus constitutes a feature that make it distinctive from the more diversified and terrestrial late-diverging fungi.

Only Cdc31p-like centrins had been identified in the fungi kingdom until 2005, when expressed sequence tags encoding two isoforms in *B. emersonii* (BeCen1 and BeCen3) were isolated and expressed [13]. This novel fact led to the question of why both

* Corresponding author. Tel.: +55 41 3361 3308.
E-mail address: camargofisico@gmail.com (P.C. de Camargo).
[1] Present address: Instituto de Agrobiotecnología del Litoral, Universidad Nacional del Litoral, CONICET, Santa Fe, Pcia. Santa Fe, Argentina.

1570-9639/$ – see front matter © 2013 Elsevier B.V. All rights reserved.
http://dx.doi.org/10.1016/j.bbapap.2013.10.007

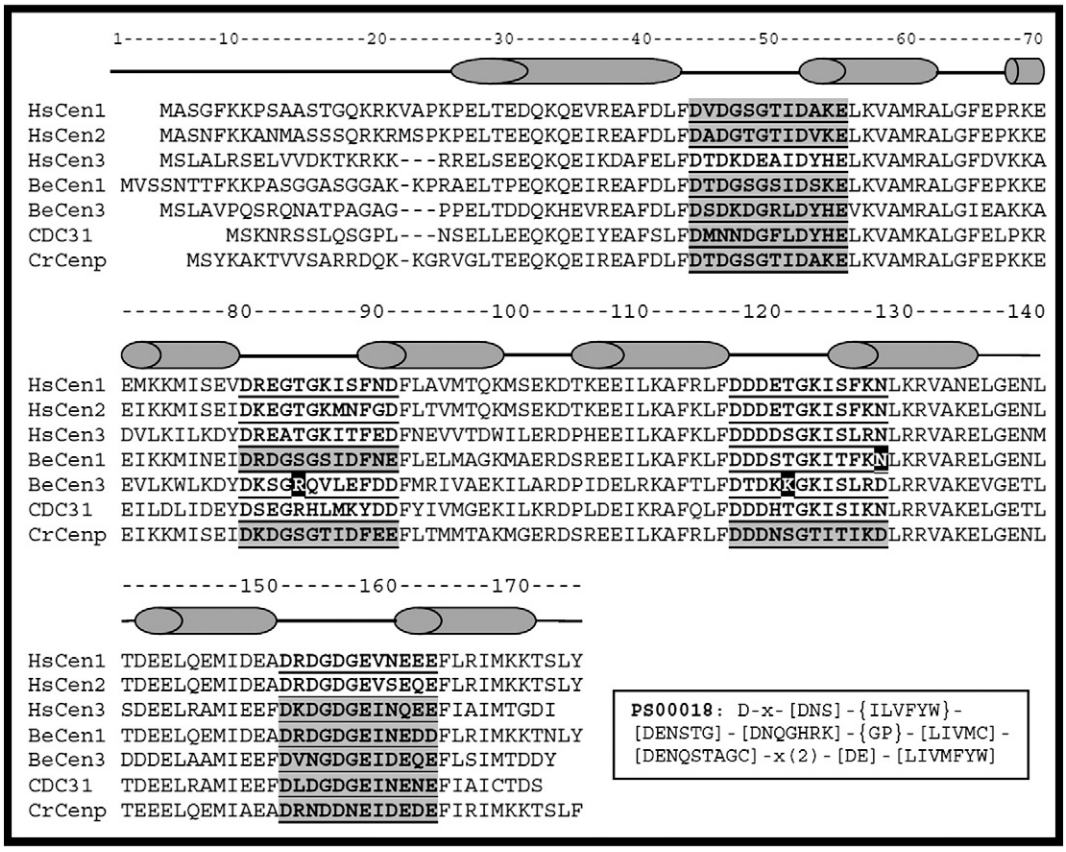

Fig. 1. Linear alignment of the centrin sequences from human (HsCen1, HsCen2 and HsCen3), *Blastocladiella emersonii* (BeCen1 and BeCen3), *Chlamydomonas reinhardtii* (CrCenp) and *Saccharomyces cerevisiae* (Cdc31p). The underlined regions indicate the EF-hand loop sequence for each protein; the gray boxes indicate the canonical calcium-binding motifs for each protein and in black boxes are the amino acids that can affect the calcium affinity for BeCen1 and BeCen3 motifs compared with pattern PS00018 from PROSITE database [19]. Based on this pattern, both BeCen1 and BeCen3 have four stretches with profiles of potential calcium-binding motifs. Secondary structure prediction was represented for a better visualization of the calcium binding loop regions (http://bioinf.cs.ucl.ac.uk/psipred/) [20].

isoforms are found in this primitive fungus and how similar these proteins are in terms of structure and function. Aiming to understand the structural differences of both isoforms, this investigation relates structural and thermodynamic features of BeCen1 and BeCen3 due to calcium binding. An examination of their self-assemble behavior by microscopic and spectroscopic methods is also provided.

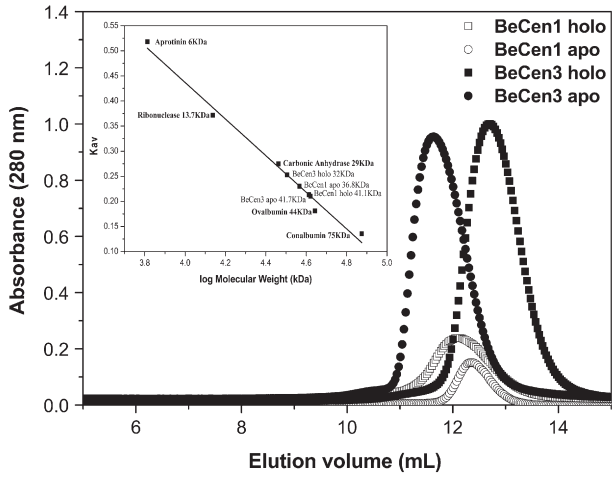

Fig. 2. Size exclusion chromatography. Elution profiles of BeCen1 and BeCen3 with and without calcium giving approximately 36.8 kDa for apo-BeCen1, 41.7 kDa for apo-BeCen3, 41.1 kDa for holo-BeCen1 and 32 kDa for holo-BeCen3. The elution volumes of standard proteins were used to calculate Kav values (inset). This data suggest that calcium ion promotes conformational changes of BeCen3 toward a more compact shape while in the case of BeCen1 it is more extended.

2. Materials and methods

2.1. Cloning, expression and purification

Complementary DNAs (cDNAs) corresponding to BeCen1 and BeCen3 were amplified through polymerase chain reaction (PCR) using a MJ Research, Inc. thermal cycler (PTC-100). BeCen1 and BeCen3 cDNAs previously cloned into pSPORT1 were used as DNA templates. For this subcloning, the primers were designed to adjoin the following regions: BeCen1-Forward-NdeI 5′ CCC ATA TGG TGT CCT CCA ACA CCA CGT TC 3′; BeCen1-Reverse-BamHI 5′ CGG ATC CTC AGT ACA GGT TGG TCT TCT TC 3′; BeCen3-Forward-NdeI 5′ GCC ATA TGT CAC TCG CGT TCC CCG TCT CGA C 3′; BeCen3-Reverse-BAMHI 5′ CGG ATC CTC AGT AGT CGT CCG TCA TGA TGC TC 3′.

The complete cDNAs encoding BeCen1 and BeCen3 were amplified, producing two fragments: 561 bp for BeCen1 and 564 bp for BeCen3. For the amplification of BeCen3, dimethyl sulfoxide (DMSO) 5% was added to the reaction.

All the amplified products and the expression vector pET28a(+) were digested with *Nde*I and *Bam*HI followed by ligation with T4 DNA ligase and transformed into DH5α *Escherichia coli*. Transformants were confirmed through PCR and restriction analysis. The new vector constructs were named pET-BeCen1 and pET-BeCen3. The fragment products were fused to a hexa histidine-tag (His-tag). All plasmids were sequenced through the dideoxy chain method using an ABI

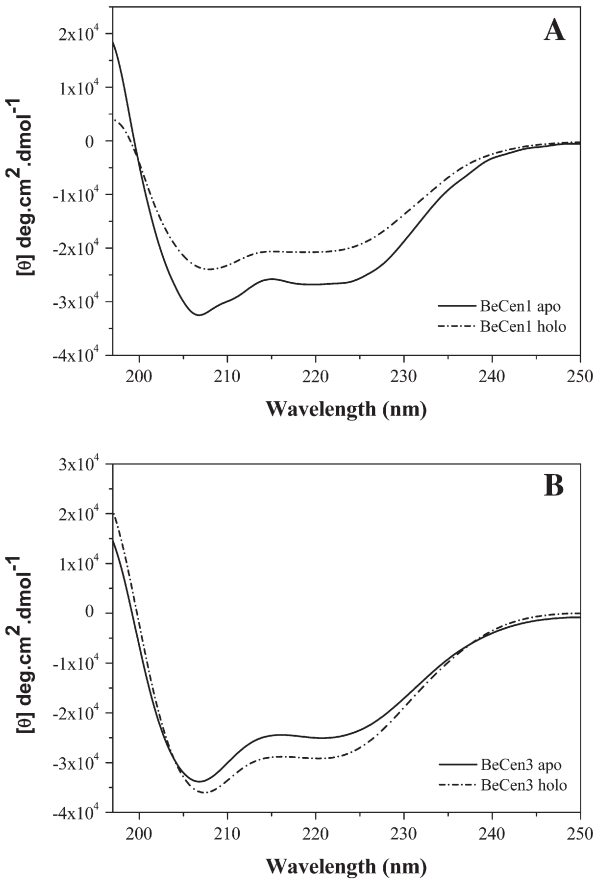

Fig. 3. Circular dichroism spectra of the apo and holo forms of BeCen1 (A) and BeCen3 (B). 0.1 mg/mL protein at 10 °C in the presence of EGTA (1 mM) or after the addition of $CaCl_2$ (2 mM). At 10 °C, the spectra of all the states are characteristic of α-helical proteins (two minima around 208 nm and 222 nm). These spectra showed a decrease in the α-helical minima (at 208 nm and 222 nm) for the holo-BeCen1 and an increase in the α-helical minima for holo-BeCen3.

Prism 377 automated DNA sequencer (PerkinElmer) following the manufacturer's protocol [14].

The expression plasmids carrying the BeCen1 and BeCen3 cDNAs were used to transform BL21(DE3) *E. coli* competent cells. A total of 500 μL of an overnight culture of BL21(DE3) carrying the pET-BeCen1 and BeCen3 plasmid was infused into 500 mL of fresh lysogeny broth (LB) medium containing kanamycin (50 μg/mL). The culture was agitated at 37 °C until an optical density of 0.6 at 600 nm was reached. Subsequently, isopropyl β-D-1-thiogalactopyranoside (IPTG) was added to a final concentration of 0.4 mM. The incubation was extended for 4 h at 37 °C followed by cell culture centrifugation. The pelleted cells were resuspended in 20 mM Tris–HCl and 10 mM NaCl (pH 7.0) buffer and disrupted adding 0.1 mg/mL lysozyme at 4 °C for 30 min followed by sonication. The suspension was then centrifuged at 18,000 ×*g* at 4 °C for 20 min and the pellet and supernatant were analyzed based on SDS-PAGE in order to check whether the proteins are in the supernatant. The supernatant containing the recombinant BeCen1 and BeCen3 was applied to a nickel-affinity column equilibrated with the same buffer. After the unbound proteins had been washed away, the recombinant protein was eluted from column by increasing the imidazole concentration to 300 mM. The recombinant BeCen1 and BeCen3 was then applied to a Superdex-75 3.2/30 size exclusion column from Pharmacia Biotech Smart System. Elution was done at 4 °C using a buffer containing 20 mM Tris–HCl and 150 mM NaCl (pH 7.0), and the fractions were analyzed using SDS-PAGE 15%. The production of purified proteins was about 5 mg/L.

The protein samples were dialyzed using a 20 mM Tris–HCl buffer (pH 7.0) containing 10 mM NaCl and 1 mM ethylene glycol tetraacetic acid (EGTA) before the assays. The protein concentration was determined using BCA Protein Assay® [15].

2.2. Size exclusion chromatography (SEC)

Calcium-induced conformational changes were investigated applying the apo and holo forms of BeCen1 and BeCen3 to a Superdex 75 3.2/30 column from Pharmacia Biotech Smart System. The column was equilibrated with a buffer containing 20 mM Tris–HCl, 150 mM NaCl and 1 mM EGTA (pH 7.0) for the apo state proteins and a buffer containing 20 mM Tris–HCl, 150 mM NaCl and 2 mM $CaCl_2$ (pH 7.0) for the holo state proteins. All protein samples (25 μM) were preincubated with 2 mM $CaCl_2$ or 1 mM EGTA at 20 °C for 2 h before being applied to the column. The chromatograms were recorded at 220 nm and 280 nm wavelengths. The relative elution volume was compared to that of the molecular mass standards. The relative elution volume was calculated using the following equation: $Kav = (Ve - Vo) / (Vg - Vo)$, where Ve is elution volume, Vo is the void volume, and Vg is the geometric column volume. A standard calibrated curve, Kav versus log molecular mass (kDa), was plotted in order to determine the apparent molecular mass of apo-BeCen1 and BeCen3 and holo-BeCen1 and BeCen3.

2.3. Circular dichroism (CD) spectroscopy

Purified BeCen1 and BeCen3 were monitored with far-UV CD spectroscopy (over a wavelength range of 197 nm to 250 nm) using a J-715 Jasco spectropolarimeter. The spectra were measured for protein concentration of 0.1 mg/mL in 20 mM Tris–HCl containing 10 mM NaCl (pH 7.0) in a 0.1 cm quartz cuvette. An average of 16 accumulations were measured, using a scanning speed of 100 nm/min, a spectral bandwidth of 1 nm, and a response time of 0.5 s. Thermal unfolding was monitored by CD spectroscopy in a temperature range from 10 °C to 90 °C at a heating rate of 1 °C per minute, by measuring changes in ellipticity at 222 nm and 208 nm. The buffer spectrum was subtracted and all experiments were performed using either 2 mM Ca^{2+} or 1 mM EGTA. The reversibility of BeCen1 and BeCen3 denaturation was assessed by acquiring the CD spectra of the sample at the same initial condition at 10 °C, after heating to 90 °C and cooling the sample overnight to 4 °C. The fraction of denaturated protein was calculated based on $fd = (\theta n - \theta obs) / (\theta n - \theta d)$, where $fn + fd = 1$; fn = fraction of native protein; θobs is the ellipticity of the sample at a specific condition, with θd and θn being the characteristic ellipticity of denatured and native states, respectively. Measurements of BeCen1 and BeCen3, under presence and in the lack of calcium were performed to identify structural changes. All the spectra were mathematically smoothed using the FFT algorithm available in Origin® 7.0.

2.4. Fluorescence experiments (ANS assay)

Fluorescence emission measurements were conducted using a spectrofluorimeter (ISS, IL, USA; model ISS K2) equipped with a refrigerated circulator (Neslab RTE-210). The excitation and emission monochromators were set at slit widths of 2 nm and 1 nm, respectively.

Fluorescent dye-binding experiments using 1-anilino-8-naphthalene-sulfonic acid (ANS) were performed to probe dynamic changes in the exposure of protein hydrophobic regions [16]. A fixed concentration of 250 μM ANS was mixed with 10 μM protein solution (20 mM Tris–HCl pH 7.0, 10 mM NaCl) in the presence or absence of final concentrations of 1 mM Ca^{2+}. The excitation wavelength was set at 360 nm, and the emission spectrum was monitored from 400 nm to 650 nm.

2.5. Isothermal titration calorimetry

Titration experiments were carried out with a VP-ITC calorimeter (MicroCal, Northampton, MA, USA). Solutions were degassed by means of a vacuum degasser (Thermo Vac, MicroCal) and thermostated

at 25 °C for 5 min prior to any experimental run. The buffer ITC solution was 20 mM Tris–HCl, 10 mM NaCl at pH 7.0. Solutions of calcium and magnesium chloride, 1 mM or 0.25 mM, were loaded in a syringe (300 μL) and titrated by 50 injections of 5 μL into a sample cell (1.43 mL) containing 6 μM of BeCen1 or 25 μM of BeCen3 with intervals of 180 s. The net heats of interaction were obtained subtracting the heats of dilution of calcium and magnesium in the buffer.

All experiments were carried out in triplicate and also repeated from different protein purifications with consistent reproducibility. Prior to binding experiments, the centrins were exhaustively dialyzed against a buffer containing 1 mM EGTA, a calcium chelating compound, to ensure proteins are Ca^{2+} free and, finally, buffer without EGTA to allow calcium protein binding.

The shape of the binding isotherm changed according to the product of the binding constant and the target concentration through the so-called c value [17], which is defined as Kb[M]n (or [M]n/Kd), where Kb is the binding constant, [M] is the macromolecule concentration and n the number of interaction sites. For accurate determination of binding constants, c values between 1 and 1000 is recommended [18]. In compliance with this recommendation, the c values in these titrations obtained for each site of proteins and Ca^{2+} varied between 1.7 and 5.

ITC curves were fitted using different binding models available in Origin® (ITC Data Analysis in Origin® Tutorial Guide Version 7.0) software. The sequential binding model that considers 4 binding sites showed the best statistical parameters and correlation with the number of calcium-binding sites prediction.

2.6. Right-angle light scattering

Samples of BeCen1 and BeCen3 (10 μM) in 20 mM Tris–HCl pH 7.0, containing 10 mM NaCl, were centrifuged (16,000 ×g at 4 °C for 10 min) and measured on a 0.5 cm path length quartz cuvette, using a spectrofluorimeter (model K2 ISS), equipped with a thermostated cuvette. The samples were illuminated with 350 nm, and the scattering light was collected at the same wavelength at 90° angle.

Measurements were made at 10 °C, 20 °C, 30 °C, 40 °C, 50 °C, and 60 °C. All intensity measurements are given in arbitrary units after deducting light scattering from the buffer.

2.7. Atomic force microscopy (AFM)

Purified BeCen1 and BeCen3 proteins (12 μM) were incubated with 1 mM EGTA or 2 mM Ca^{2+} at 50 °C for 60 min. For AFM measurements, samples were prepared on recently cleaved mica slices by dip-coating in 12 μM protein solution at 50 °C and let to dry, at 40% humidity, for 48 h at 36 °C. AFM images were obtained at room temperature (25 °C), using a Shimadzu 9500J equipment operating in dynamic mode, with ultra-sharp Nanosensor cantilever of approximately 2 nm tip radius and 40 N/m spring constant, at scanning rate of 1 Hz. Interaction parameters, such as, operating point and oscillation amplitude were adjusted to minimize interaction and optimize image quality.

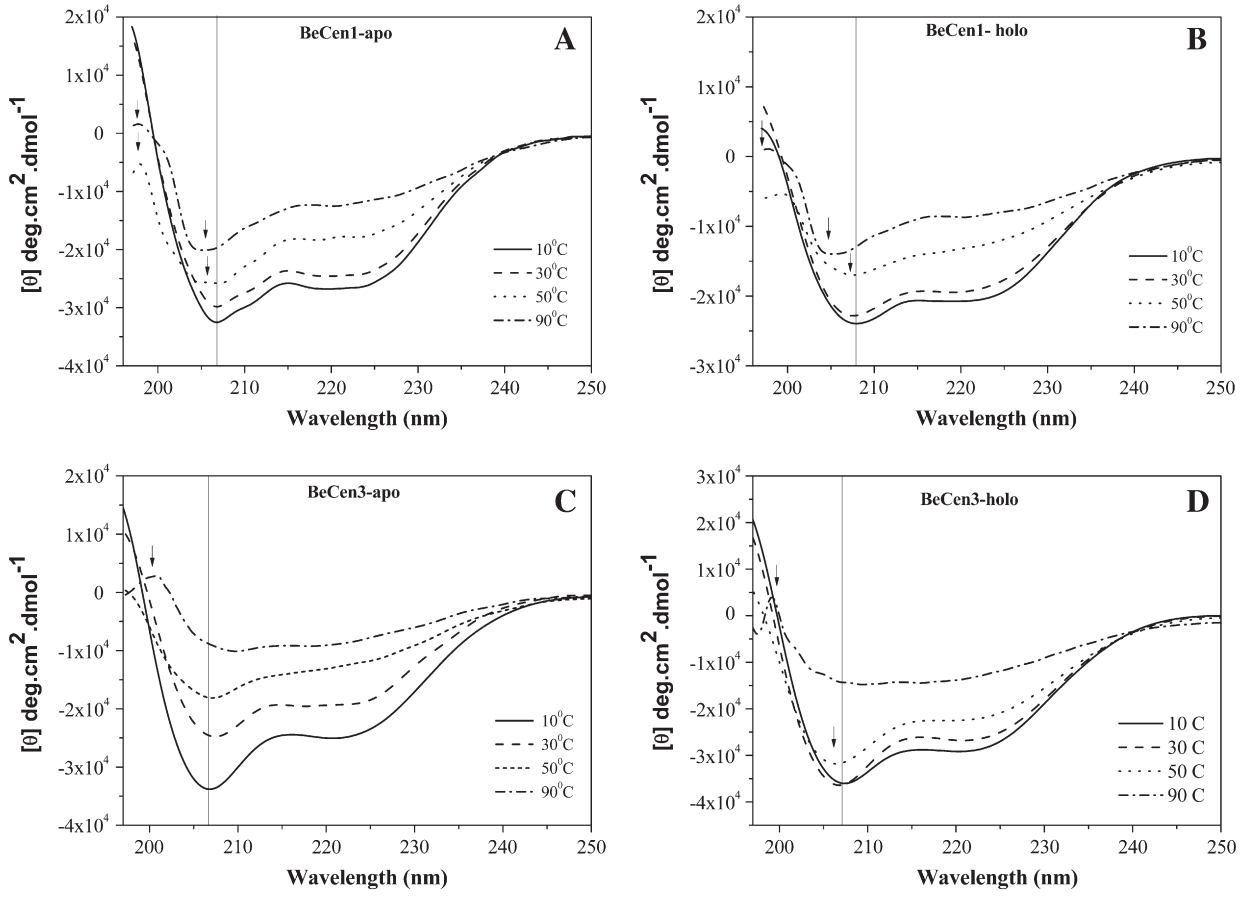

Fig. 4. Thermal unfolding of BeCen1 and BeCen3. Circular dichroism (CD) spectra as a function of temperature were recorded in 20 mM Tris–HCl pH 7.0, containing 10 mM NaCl with 2 mM $CaCl_2$ or 1 mM EGTA in the temperature range from 10 to 90 °C (Tm was achieved taking account individual spectra into this temperature range). (A) BeCen1 with EGTA, (B) BeCen1 with $CaCl_2$, (C) BeCen3 with EGTA and (D) BeCen3 with $CaCl_2$. As the temperature increases (above 30 °C), the characteristic minima at 208 nm and 222 nm become less evident for both proteins. In the apo form Tm is 42 °C for BeCen1 and 49 °C for BeCen3, while in the holo form Tm is 46 °C for BeCen1 and 54 °C for BeCen3.

3. Results and discussion

3.1. Cloning, expression and purification of centrins

DNA amplifications produced fragments of 561 bp and 564 bp corresponding to the encoding region of BeCen1 and BeCen3, respectively. The expression vectors containing the inserts were used to transform *E. coli* BL21(DE3). After induction with IPTG, *E. coli* cells harboring pET-BeCen1 and pET-BeCen3 produced additional bands corresponding to BeCen1 and BeCen3 added to the N-terminal 6His-tag. The largest portion of expression product was found in the supernatant after lysis. After Ni-NTA affinity purification, the products were further purified through SEC using a Superdex-75 column. Final yields were typically 5 mg/L protein of culture medium for both BeCen1 and BeCen3 (Fig. S1, Supplementary material).

Fig. 1 shows the alignment of human centrins 1, 2, and 3; BeCen1 and BeCen3, yeast centrin Cdc31p from *S. cerevisiae* and green algae centrin CrCenp from *C. reinhardtii*. The sequences of the four EF-hand motifs are highlighted in bold and underlined while the canonical calcium binding motifs are emphasized in gray.

Analyzing the amino acid residues located in the EF-hand loop region, and using the ScanProsite tool (http://prosite.expasy.org/scanprosite/) to find the pattern for calcium binding domains, one can notice that both BeCen1 and BeCen3 have four stretches with profiles of potential calcium-binding motifs matching the pattern PS00018 [19]. BeCen1 has three sites that fulfill the canonical pattern observed in typical EF-hand motifs PS00018, while BeCen3 has only two. BeCen1 has an asparagine (N) in the position 12 in the third site, also observed in SdCen/skMLCK complex from *Scherffelia dubia* (PDB ID: 3kf9), which binds four calcium molecules and shares 83% of identity with BeCen1 [21]. BeCen3 has an arginine (R) in the position 5 at the second site and a lysine (K) in the position 5 at the third site, which does not match any canonical EF-hand pattern.

The 6th residue in an EF-hand loop, in most cases, is a glycine (G) due to the conformational requirements of the backbone [10]; however, there are a number of exceptions to this 'rule'. BeCen3 is one of these exceptions since it has a glutamine (Q) in this position at the second site. The comparison of sequence alignment between BeCen1, BeCen3 and EF-hand domains indicates that these proteins have structural differences, leading to different calcium binding recognition (Fig. 1).

The sequence analysis of both centrins shows that BeCen1 shares its highest identity with the centrins HsCen1 (70%), HsCen2 (70%) and CrCenp (72%), which are responsible for contractile functions (7). Therefore, the presence of BeCen1 can be associated to contractile functions of the flagellar stage in *B. emersonii* life cycle. On the other hand, BeCen3 has its highest identity with HsCen3 (52%) and Cdc31p (53%), which are responsible for MTOC duplication [7]. Moreover, BeCen1 and BeCen3 share only 44% identity.

Motivated by the differences in primary structures of BeCen1 and BeCen3, physical methods were performed to identify structural and thermodynamic differences between these proteins.

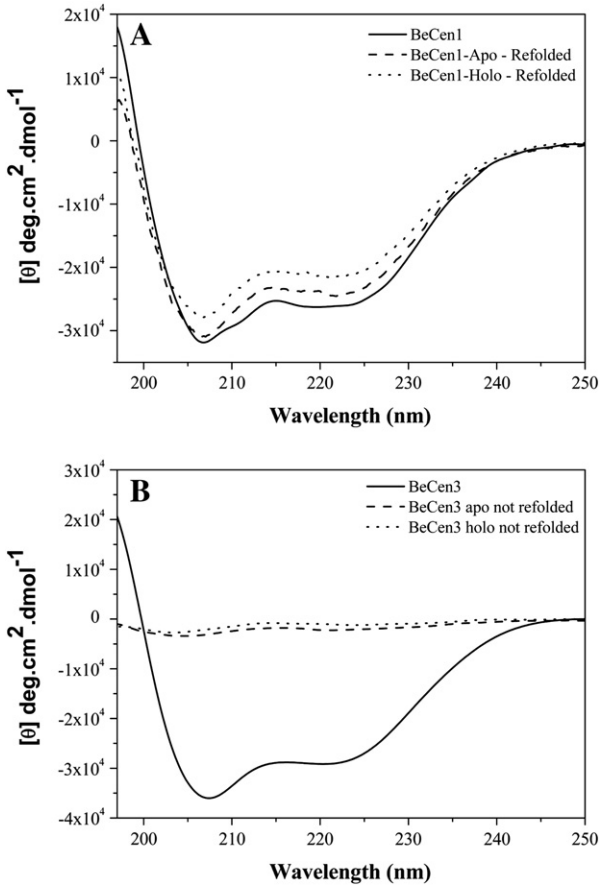

Fig. 5. Circular dichroism spectra of the BeCen1 and BeCen3 refolding processes. (A) BeCen1 and (B) BeCen3. At 90 °C, both proteins were denaturated, however, after being cooled overnight to 4 °C both forms of BeCen1 refolded, contrasting with both forms of BeCen3.

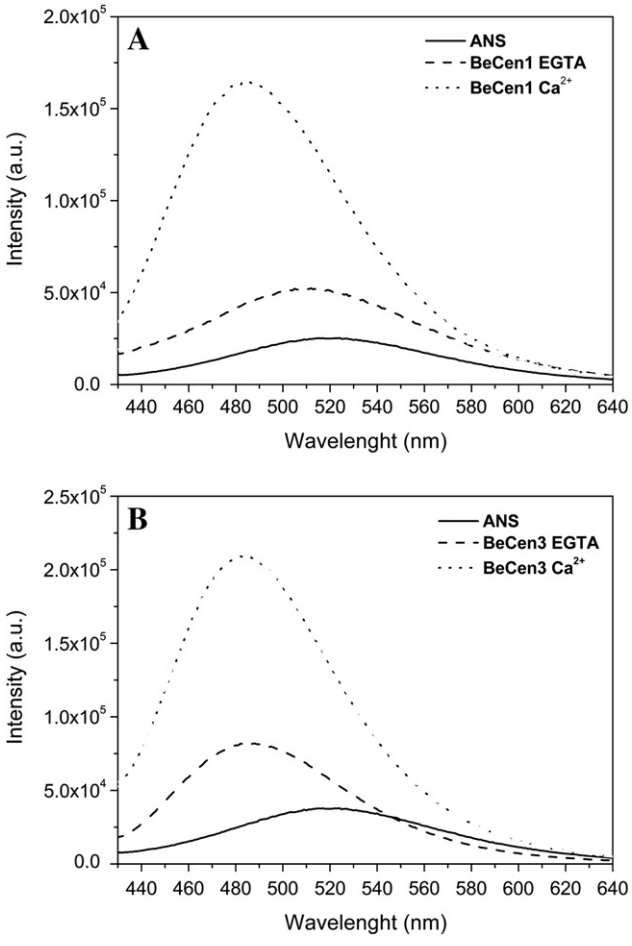

Fig. 6. Fluorescence emission of ANS probe. Conformational changes in: (A) BeCen1 with and without calcium and (B) BeCen3 with and without calcium. The addition of calcium causes an intensity increase similar for both proteins, likely due to hydrophobic exposure. Taking ANS fluorescence as a reference, apo-BeCen1 shows a slight blue shift to approximately 512 nm, while apo-BeCen3 added to ANS causes a larger blue shift to approximately 483 nm.

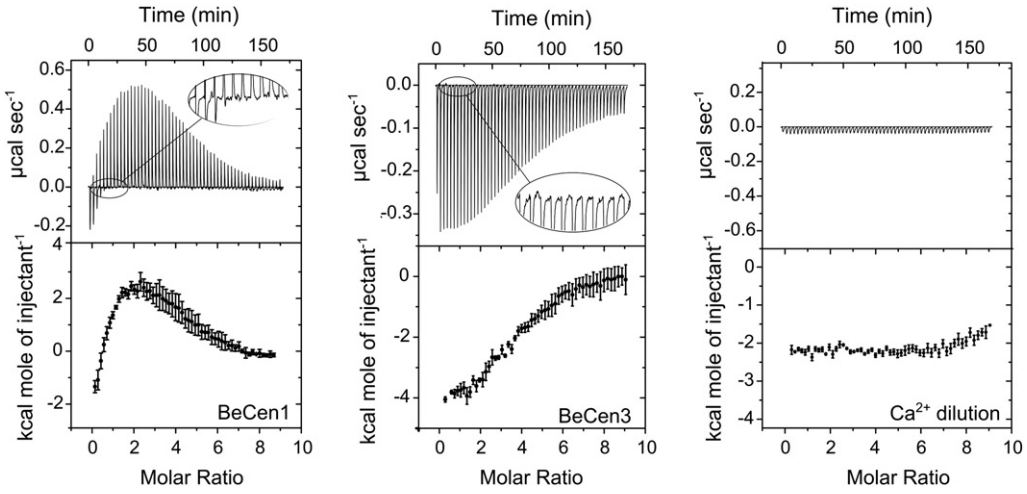

Fig. 7. Calcium binding observed by isothermal titration calorimetry. Thermograms (top panels) and isotherms (bottom panels) of the titration of Ca^{2+} (1 mM) into 25 μM BeCen1 (left), Ca^{2+} (0.25 mM) into 6 μM BeCen3 (middle), Ca^{2+} dilution (right) at 25 °C. Binding of the first, second, third and fourth calcium ion occurs with an average of the given affinities. Experiments were carried out in triplicate.

3.2. Size exclusion chromatography upon calcium addition

As shown in Fig. 2 the apparent molecular mass for holo-BeCen1 appeared as a single peak at 41.1 kDa while, for apo-BeCen1, it was found at 36.8 kDa (real molecular mass being 22.1 kDa). Calcium has an opposite effect on BeCen3, where the apparent molecular mass of apo-BeCen3 is 41.7 kDa and 32 kDa for holo-BeCen3 (real molecular mass being 22.9 kDa). The elution time depends on the macromolecular conformation and interactions with the chromatography column. Therefore, for elongated shape centrins, SEC delivers 1.7 more mass than the real molecular mass [22].

Taking into account the retention time, calcium is likely to promote conformational changes of BeCen3 toward a more compact shape, when compared to an extended shape for BeCen1. According to a similar study using SEC [22], a compaction was also suggested for centrin Cdc31p from *S. cerevisiae* (53% of identity with BeCen3). BeCen1 presented a smaller difference in the elution position due to calcium, suggesting less structural rearrangement than BeCen3. This behavior is similar to that reported for centrins HsCen1 and HsCen2 (70% of identity with BeCen1), which do not seem to alter their conformational shape after calcium addition [22].

3.3. Changes of secondary structure are triggered by calcium

CD spectra were analyzed in order to compare the conformational changes triggered by calcium in both centrins. These spectra showed a decrease in the α-helical minima (at 208 nm and 222 nm) for the holo-BeCen1 (Fig. 3A) and an increase in the α-helical minima for holo-BeCen3 (Fig. 3B). Similar results have been described for human centrin HsCen1 (70% identity with BeCen1), in which the holo form showed a decrease in the α-helical minima, while yeast centrin Cdc31p (53% identity with BeCen3) showed an increase in α-helical minima for the holo form [22].

The structural changes of apo and holo BeCen1 and BeCen3, investigated by CD spectroscopy from 10 °C to 90 °C, kept the two negative minima around 208 nm and 222 nm that are characteristic of α-helical proteins (Fig. 4). As the temperature increases (above 30 °C), the characteristic minima at 208 nm and 222 nm become less evident for both proteins. In the apo form, the mean transition temperature (Tm) determined at the inflection point on the plot of denaturated protein fraction against temperature, gives 42 °C for BeCen1 and 49 °C for BeCen3. In the holo form, the same procedure leads to Tm of 46 °C for BeCen1 and 54 °C for BeCen3.

Additionally, around 50 °C, there was a tendency of a blue shift in the CD minima and a decrease in the positive maximum intensity (around 198 nm) suggesting changes in secondary structures for both proteins. At 90 °C, both proteins were denaturated, however, after being cooled overnight to 4 °C, both forms of BeCen1 refolded (Fig. 5A). It is worth noting that calcium added to HsCen1 behaves similarly to BeCen1 [22]. BeCen3 did not present relevant changes in its denaturated CD spectrum after cooling, showing an irreversible denaturation either with or without calcium (Fig. 5B).

3.4. Exposure of hydrophobic regions monitored by ANS fluorescence

In order to compare the exposure of hydrophobic patches for calcium free and calcium loaded proteins, an extrinsic ANS probe was used. When ANS forms a complex with the target protein, two effects are likely to occur: the exposure of hydrophobic regions increasing emission intensity and a blue shift due to mechanism associated to conformational changes [23].

Fig. 6 provides a comparison of the emission spectrum between free ANS, excited at 380 nm with maximum intensity at 521 nm, and ANS associated with apo and holo forms of both proteins. The main feature of these results, taken ANS emission as a reference, is that both apo-BeCen1 and apo-BeCen3 caused a 2-fold maximum intensity increase

Table 1
Thermodynamic parameters for Ca^{2+} binding to BeCen1. Binding affinities refer to the average affinity for the first, second, third and fourth calcium bound, not to the affinity of the individual sites.

BeCen1	Site 1	Site 2	Site 3	Site 4
K_d (μM)	6.06 ± 2.26	7.50 ± 0.44	75.20 ± 28.3	9.35 ± 0.93
ΔG (kcal mol^{-1})	−7.13 ± 0.23	−6.98 ± 0.03	−5.64 ± 0.23	−6.86 ± 0.06
ΔH (kcal mol^{-1})	−3.82 ± 1.08	9.12 ± 0.85	2.72 ± 1.48	3.06 ± 1.48
TΔS (kcal mol^{-1})	−3.31	−16.10	−8.36	−9.92

Table 2
Thermodynamic parameters for Ca^{2+} binding to BeCen3. Binding affinities refer to the average affinity for the first, second, third and fourth calcium bound, not to the affinity of the individual sites.

BeCen3	Site 1	Site 2	Site 3	Site 4
K_d (μM)	2.45 ± 0.04	18.5 ± 0.86	2.11 ± 0.38	38.1 ± 7.46
ΔG (kcal mol^{-1})	−7.65 ± 0.01	−6.45 ± 0.03	−7.73 ± 0.10	−6.02 ± 0.11
ΔH (kcal mol^{-1})	−5.28 ± 0.83	−11.53 ± 1.98	−2.75 ± 1.55	0.73 ± 0.09
TΔS (kcal mol^{-1})	−2.37	5.08	−4.98	−6.75

(Fig. 6A and B, respectively). On the other hand, apo-BeCen1 showed a slight blue shift to approximately 512 nm, while apo-BeCen3 added to ANS caused a larger blue shift to approximately 483 nm, suggesting that the exposure of hydrophobic surface is more pronounced for apo-BeCen3 and ANS. Otherwise, the maximum emission intensity increases approximately 7 times for holo-BeCen1 and 6 times for holo-BeCen3. It is worthwhile to notice that calcium causes an intensity increase similar for both proteins, likely due to hydrophobic exposure. However, for BeCen3 the large blue shift from 521 nm to 483 nm is probably partly the result of charge transfer and may be associated to positively charged amino acids, like lysine present in the position 5 at the third calcium binding site in the BeCen3 [24].

It is known that calcium may cause exposure of hydrophobic residues promoting the binding of these proteins to other proteins and to molecules, or even contributing to a self-assembly process when needed [25].

3.5. BeCen1 and BeCen3 have 4 calcium binding sites, with very different profiles

In order to investigate the thermodynamic parameters of centrins upon calcium and magnesium binding, isothermal titration calorimetry (ITC) was used. Binding experiments of centrins were carried out with calcium and magnesium searching for its distinct roles [26]. Thermograms of BeCen1 and BeCen3 for calcium binding showed mainly endothermic and exothermic profiles respectively (Fig. 7).

Isotherms were fitted using all models of Origin® and the sequential four binding site model resulted in the best experimental data fitting for both proteins (for more details of the analysis see the Supplementary material — Fig. S3, S4 and Tables S1 and S2). In the literature there are centrins with less calcium binding sites, but also centrins from different organism with four binding sites [27–29].

The number of potential binding sites predicted by Prosite Tool, as discussed in Section 3.1, confirmed four binding sites. The diversity of amino acid composition of the EF-hand motifs and the cooperativity process are commonly observed for EF-hand domains [19], pointing to the need of individual site analysis (see the thermodynamic parameters in Tables 1 and 2), although the binding constants cannot be associated directly with individual sites as reported by Linse et. al. [30]. In this way, binding affinity correspond to an average of calcium ion binding affinity of all available binding sites with unknown degree of cooperativity. Therefore, taking into account a sequential effective binding regime, neglecting cooperativity for comparison purpose, BeCen1 is considered to have three regimes (similar Kd) with comparable affinity and one 10 fold lower for BeCen1, while BeCen3 has two regimes with Kd of 2 μM and two with lower affinity, 18 μM and 38 μM. BeCen3 is similar to calmodulin concerning calcium binding affinity, where two calcium affinity constants are significantly higher than the other two, suggesting a bind in a semisequential manner [30]. Surprisingly, no evidence of magnesium binding was detected within the resolution of ITC (see Fig. S2 — Supplementary material), suggesting that both BeCen1 and BeCen3 are calcium signaling selective.

Favorable entropy of metal binding to EF-hand domain is mainly a result of water molecules release from protein binding site and unfavorable entropy is usually associated with constraints of the loop flexibility, conformational changes and exposure of hydrophobic surfaces. Enthalpy changes upon calcium binding are a sum of different contributions. Favorable contributions are observed, when electrostatics interactions are established between the metal and carboxylated side chains while dehydration of metal ions and interhelical interactions (for proteins that undergo large calcium-induced conformational change) present unfavorable contributions [10].

BeCen1 ITC binding curve is biphasic with positive enthalpy while BeCen3 has a unique phase with negative enthalpy. CD-signal shows a gain in helix content for BeCen3 and losses for BeCen1; SEC experiments suggests a compaction of BeCen3 and a small extension of BeCen1, clearly demonstrating opposite behaviors of these centrins upon calcium binding. Differences on thermodynamic parameters may arise from different structure rearrangements as observed in HsCen3 [26].

3.6. Formation of high order particles in solution

Right-angle light scattering (RALS) was used to investigate the ability of BeCen1 and BeCen3 to form aggregates and filaments, phenomena already described for centrins, as a consequence of increasing temperature and $CaCl_2$ addition [25]. Measurements performed at 340 nm indicated that BeCen1 and BeCen3 aggregate possibly going through a filamentous state above certain temperatures (Fig. 8A and B). These results are similar to the finding for the human centrin HsCen2 [25]. However, after analyzing calcium effects in both systems it is clear that the two proteins have different features. The presence of calcium does not affect the light scattering for BeCen1 (Fig. 8A), contrasting with the scattering intensity for apo-BeCen3 that starts at approximately 40 °C while for the holo state, the transition occurs at 30 °C. In the case of holo-BeCen3, the increase in Tm upon calcium binding established by CD, is in an apparent contrast with RALS results. However, the increase in light scattering can be due to the formation of larger particles compared to the apo form, since the extent of scattering also depends on the particle size. The irreversibility of BeCen3 thermal denaturation also indicates that larger aggregates are formed.

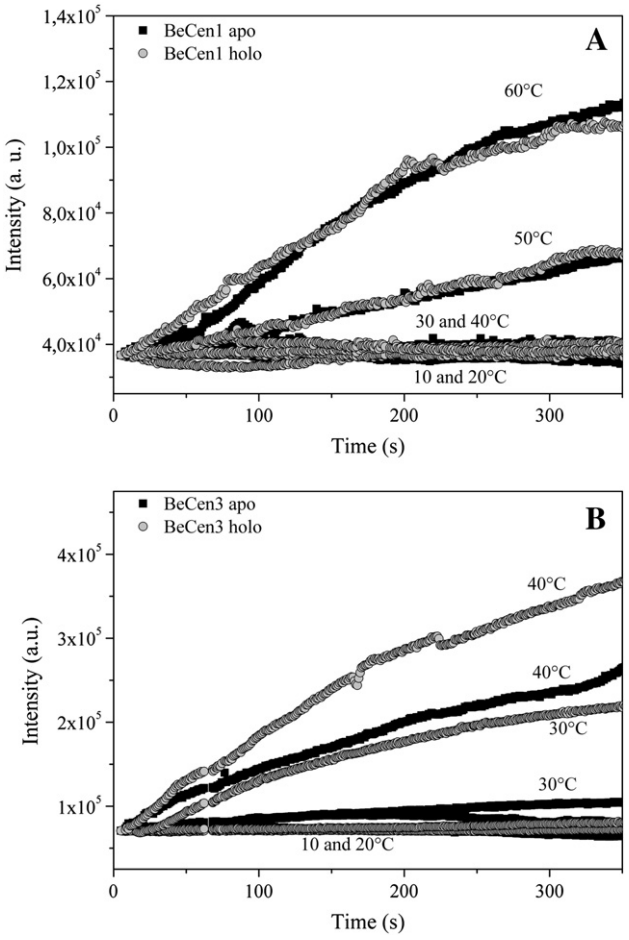

Fig. 8. Right angle light scattering of (A) BeCen1 and (B) BeCen3 as a function of temperature. Scattering intensity at 340 nm was measured as a function of time at each temperature for the samples (40 μM protein) in 20 mM Tris–HCl, 10 mM NaCl and with 2 mM calcium or 1 mM EGTA (pH 7.0). Calcium does not affect the light scattering for BeCen1, contrasting with the scattering intensity for apo-BeCen3 that starts at approximately 40 °C, while for the holo state the transition occurs at 30 °C.

3.7. Apo BeCen1 and Apo BeCen3 filaments were visualized by atomic force microscopy

Despite of evidences that BeCen1 and BeCen3 aggregate at certain temperatures, further experiments are needed to investigate the form and size of these supramolecules. Therefore, AFM was used searching for evidences of filament formation. Fig. 9 shows filaments of approximately 150 nm wide and micrometers long for apo-BeCen1 and apo-BeCen3. Interestingly, regular but no filamentary structures were observed in the holo forms (data not shown).

Details of selected and typical BeCen1 and BeCen3 filamentary structures are shown (Fig. 9A and B), where the filamentary structures appear across the substrate.

Typical filamentary structures observed for BeCen1 and BeCen3 are shown in Fig. 9A and B. The filaments formed by apo-BeCen3 are oriented in an apparently coiled and compact structure, with dimensions around 150 nm wide and 23 nm high. Apo-BeCen1 presented branches apparently less compact, suggesting the presence of different interaction sites and forming bundles of filaments around 200 nm wide and about 50 nm high. The similarities of calcium binding effects between HsCen2 and BeCen1 and also between Cdc31p and BeCen3 are consistent with the expectation that relevant differences on the filamentary structure between BeCen1 and BeCen3 may contribute to putative different biological roles [22].

This is the first direct observation of filamentary structures formed just by centrins in the absence of calcium. An example of centrin filament formed without calcium, however not self assemble, was reported by Li et al. [31] using transmission electron microscopy on Cdc31p combined with protein Sfi1 forming a complex with roughly 60 nm-diameter.

Filamentary formation has been well documented for so many proteins [32,33] that it was proposed as a universal property of proteins. Despite of not being well established yet, the fibrils found for the apo forms of BeCen1 and BeCen3 (Fig. 9) follow a general trend of protein filamentary formation, but not being amyloids (Thioflavin-T, a specific probe to detect amyloid structures, was used as described previously [34] and no amyloid fibrils were detected — data not shown).

4. Conclusions

A protocol for production, expression and purification of BeCen1 and BeCen3 centrins from *B. emersonii* was established, allowing structural and thermodynamic characterization. Amino acid sequences allow the classification of BeCen1 in the group of contractile function EF-hand centrins (HsCen1, HsCen2 and CrCenp), whereas BeCen3 in the group of microtubule organizing center (MTOC) proteins like HsCen3 and Cdc31p. Regarding the fact that both isoforms are found in this primitive

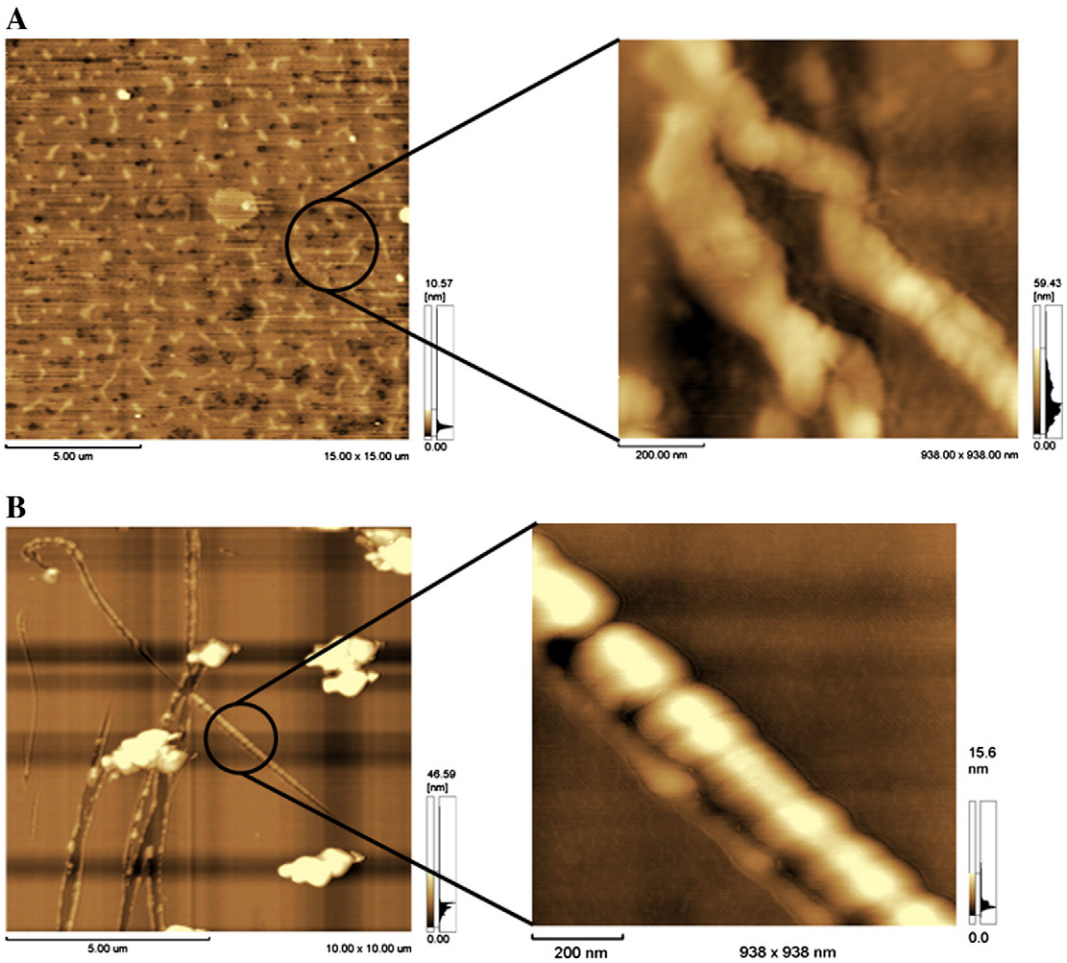

Fig. 9. AFM images — tapping mode: (A) apo-BeCen1 and (B) apo-BeCen3. Samples were prepared on cleaved mica slices by dip-coating in 12 μM protein solution at 50 °C and left to dry, at 40% humidity, for 48 h at 36 °C. The filaments formed by apo-BeCen3 are oriented in an apparently coiled and compact structure, with dimensions around 150 nm wide and 23 nm high. Apo-BeCen1 presented branches apparently less compact, suggesting the presence of different interaction sites and forming bundles of filaments around 200 nm wide and about 50 nm high.

fungus, structural and thermodynamic calcium binding investigations showed very distinct response under similar conditions.

ITC experimental results identified four calcium binding sites for both proteins, however, BeCen1 being mostly endothermic and biphasic contrasting with BeCen3, which is mainly exothermic and single phase. Under the same parameters, ITC is not sensitive to detect magnesium binding. Although four calcium binding sites were identified for both proteins, calcium ion promotes an extension in BeCen1 (SEC) with enthalpically unfavorable binding, suggesting the disruption of molecular interactions (ITC) and also a decrease in α-helix CD signal. Contrasting, upon calcium binding BeCen3 showed a more compacted form (SEC) with favorable enthalpy corresponding to a folding process (ITC) and an increase in α-helix CD signal.

Despite the relevant structural and thermodynamic differences between BeCen1 and BeCen3, the precise conditions of filamentary formation of these and many other centrins remain to be established. This investigation represents the first step toward understanding the relationship between these proteins, their main differences and centrin filament formation as viewed through AFM.

In summary, significant structural and thermodynamic features and differences between both isoforms were established; however, specific functional investigation is required to correlate the physical features with their roles in the fungi.

Supplementary data related to this article can be found online at http://dx.doi.org/10.1016/j.bbapap.2013.10.007.

Acknowledgements

The present study was supported by a grant awarded by FAPESP and partially supported by a grant from CNPq and Capes. We also thank Professor Suely Lopes Gomes for providing the BeCen1 and BeCen3 DNA used in this research.

References

[1] T.C. Meng, S.B. Aley, S.G. Svard, M.W. Smith, B. Huang, J. Kim, F.D. Gillin, Immunolocalization and sequence of caltractin/centrin from the early branching eukaryote *Giardia lamblia*, Mol. Biochem. Parasitol. 79 (1996) 103–108.
[2] M.A. Sanders, J.L. Salisbury, Centrin plays an essential role in microtubule severing during flagellar excision in *Chlamydomonas reinhardtii*, J. Cell Biol. 124 (1994) 795–805.
[3] P. Baum, C. Furlong, B. Byers, Yeast gene required for spindle pole body duplication: homology of its product with Ca^{2+}-binding proteins, Proc. Natl. Acad. Sci. U. S. A. 83 (1986) 5512–5516.
[4] J.K. Zhu, R.A. Bressan, P.M. Hasegawa, An *Atriplex nummularia* cDNA with sequence relatedness to the algal caltractin gene, Plant Physiol. 99 (1992) 1734–1735.
[5] V.D. Lee, B. Huang, Molecular cloning and centrosomal localization of human caltractin, Proc. Natl. Acad. Sci. U. S. A. 90 (1993) 11039–11043.
[6] R. Errabolu, M.A. Sanders, J.L. Salisbury, Cloning of a cDNA encoding human centrin, an EF-hand protein of centrosomes and mitotic spindle poles, J. Cell Sci. 107 (Pt 1) (1994) 9–16.
[7] S. Middendorp, A. Paoletti, E. Schiebel, M. Bornens, Identification of a new mammalian centrin gene, more closely related to *Saccharomyces cerevisiae* CDC31 gene, Proc. Natl. Acad. Sci. U. S. A. 94 (1997) 9141–9146.
[8] A. Pulvermuller, A. Giessl, M. Heck, R. Wottrich, A. Schmitt, O.P. Ernst, H.W. Choe, K.P. Hofmann, U. Wolfrum, Calcium-dependent assembly of centrin–G-protein complex in photoreceptor cells, Mol. Cell. Biol. 22 (2002) 2194–2203.
[9] M. Araki, C. Masutani, M. Takemura, A. Uchida, K. Sugasawa, J. Kondoh, Y. Ohkuma, F. Hanaoka, Centrosome protein centrin 2/caltractin 1 is part of the xeroderma pigmentosum group C complex that initiates global genome nucleotide excision repair, J. Biol. Chem. 276 (2001) 18665–18672.
[10] J.L. Gifford, M.P. Walsh, H.J. Vogel, Structures and metal-ion-binding properties of the Ca^{2+}-binding helix-loop-helix EF-hand motifs, Biochem. J. 405 (2007) 199–221.
[11] T.Y. James, P.M. Letcher, J.E. Longcore, S.E. Mozley-Standridge, D. Porter, M.J. Powell, G.W. Griffith, R. Vilgalys, A molecular phylogeny of the flagellated fungi (Chytridiomycota) and description of a new phylum (Blastocladiomycota), Mycologia 98 (2006) 860–871.
[12] J.S. Lovett, Growth and differentiation of the water mold *Blastocladiella emersonii*: cytodifferentiation and the role of ribonucleic acid and protein synthesis, Bacteriol. Rev. 39 (1975) 345–404.
[13] K.F. Ribichich, S.L. Gomes, *Blastocladiella emersonii* expresses a centrin similar to *Chlamydomonas reinhardtii* isoform not found in late-diverging fungi, FEBS Lett. 579 (2005) 4355–4360.
[14] F. Sanger, S. Nicklen, A.R. Coulson, DNA sequencing with chain-terminating inhibitors, Proc. Natl. Acad. Sci. U. S. A. 74 (1977) 5463–5467.
[15] P.K. Smith, R.I. Krohn, G.T. Hermanson, A.K. Mallia, F.H. Gartner, M.D. Provenzano, E.K. Fujimoto, N.M. Goeke, B.J. Olson, D.C. Klenk, Measurement of protein using bicinchoninic acid, Anal. Biochem. 150 (1985) 76–85.
[16] G.V. Semisotnov, N.A. Rodionova, O.I. Razgulyaev, V.N. Uversky, A.F. Gripas, R.I. Gilmanshin, Study of the "molten globule" intermediate state in protein folding by a hydrophobic fluorescent probe, Biopolymers 31 (1991) 119–128.
[17] W.B. Turnbull, A.H. Daranas, On the value of c: can low affinity systems be studied by isothermal titration calorimetry? J. Am. Chem. Soc. 125 (2003) 14859–14866.
[18] M.M. Pierce, C.S. Raman, B.T. Nall, Isothermal titration calorimetry of protein–protein interactions, Methods 19 (1999) 213–221.
[19] Y. Zhou, W. Yang, M. Kirberger, H.W. Lee, G. Ayalasomayajula, J.J. Yang, Prediction of EF-hand calcium-binding proteins and analysis of bacterial EF-hand proteins, Proteins 65 (2006) 643–655.
[20] D.T. Jones, Protein secondary structure prediction based on position-specific scoring matrices, J. Mol. Biol. 292 (1999) 195–202.
[21] Y.L. Wang, K.J. Addess, J. Chen, L.Y. Geer, J. He, S.Q. He, S.N. Lu, T. Madej, A. Marchler-Bauer, P.A. Thiessen, N.G. Zhang, S.H. Bryant, MMDB: annotating protein sequences with Entrez's 3D-structure database, Nucleic Acids Res. 35 (2007) D298–D300.
[22] H. Wiech, B.M. Geier, T. Paschke, A. Spang, K. Grein, J. Steinkotter, M. Melkonian, E. Schiebel, Characterization of green alga, yeast, and human centrins — specific subdomain features determine functional diversity, J. Biol. Chem. 271 (1996) 22453–22461.
[23] A.C. Saucier, S. Mariotti, S.A. Anderson, D.L. Purich, Ciliary dynein conformational changes as evidenced by the extrinsic fluorescent probe 8-anilino-1-naphthalenesulfonate, Biochemistry-Us 24 (1985) 7581–7585.
[24] D. Matulis, R. Lovrien, 1-Anilino-8-naphthalene sulfonate anion-protein binding depends primarily on ion pair formation, Biophys. J. 74 (1998) 422–429.
[25] M. Tourbez, C. Firanescu, A. Yang, L. Unipan, P. Duchambon, Y. Blouquit, C.T. Craescu, Calcium-dependent self-assembly of human centrin 2, J. Biol. Chem. 279 (2004) 47672–47680.
[26] J.A. Cox, F. Tirone, I. Durussel, C. Firanescu, Y. Blouquit, P. Duchambon, C.T. Craescu, Calcium and magnesium binding to human centrin 3 and interaction with target peptides, Biochemistry-Us 44 (2005) 840–850.
[27] R. Chattopadhyaya, W.E. Meador, A.R. Means, F.A. Quiocho, Calmodulin structure refined at 1.7 A resolution, J. Mol. Biol. 228 (1992) 1177–1192.
[28] T.A. Craig, L.M. Benson, H.R. Bergen, S.Y. Venyaminov, J.L. Salisbury, Z.C. Ryan, J.R. Thompson, J. Sperry, M.L. Gross, R. Kumar, Metal-binding properties of human centrin-2 determined by micro-electrospray ionization mass spectrometry and UV spectroscopy, J. Am. Soc. Mass Spectrom. 17 (2006) 1158–1171.
[29] L.A. Duan, W. Liu, Z.J. Wang, A.H. Liang, B.S. Yang, Critical role of tyrosine 79 in the fluorescence resonance energy transfer and terbium(III)-dependent self-assembly of ciliate *Euplotes octocarinatus* centrin, J. Biol. Inorg. Chem. 15 (2010) 995–1007.
[30] S. Linse, A. Helmersson, S. Forsen, Calcium-binding to calmodulin and its globular domains, J. Biol. Chem. 266 (1991) 8050–8054.
[31] S. Li, A.M. Sandercock, P. Conduit, C.V. Robinson, R.L. Williams, J.V. Kilmartin, Structural role of Sfi1p–centrin filaments in budding yeast spindle pole body duplication, J. Cell Biol. 173 (2006) 867–877.
[32] A.K. Chamberlain, C.E. MacPhee, J. Zurdo, L.A. Morozova-Roche, H.A.O. Hill, C.M. Dobson, J.J. Davis, Ultrastructural organization of amyloid fibrils by atomic force microscopy, Biophys. J. 79 (2000) 3282–3293.
[33] R. Khurana, C. Ionescu-Zanetti, M. Pope, J. Li, L. Nielson, M. Ramirez-Alvarado, L. Regan, A.L. Fink, S.A. Carter, A general model for amyloid fibril assembly based on morphological studies using atomic force microscopy, Biophys. J. 85 (2003) 1135–1144.
[34] J.C. Pissuti Damalio, W. Garcia, J.N. Alves Macedo, I. de Almeida Marques, J.M. Andreu, R. Giraldo, R.C. Garratt, A.P. Ulian Araujo, Self assembly of human septin 2 into amyloid filaments, Biochimie 94 (2011) 628–636.